Automatic quantification of viability in epithelial cell cultures by texture analysis

N. MALPICA*, A. SANTOS*, A. TEJEDOR†, A. TORRES†,
M. CASTILLA†, P. GARCÍA-BARRENO† & M. DESCO†

*Departamento de Ingeniería Electrónica, ETSI Telecomunicación Universidad Politécnica de Madrid
Ciudad Universitaria s/n, E-28040, Madrid, Spain*

†*Medicina Experimental, Hospital General Universitario 'Gregorio Marañón' C/Dr Esquerdo,
46 E-28007 Madrid, Spain*

Summary

Quantification of live cells in phase contrast microscopy images allows *in vivo* assessment of the viability of cultured cells. An automatic screening procedure seems advisable because of the large number of cells that must be counted to achieve reasonable accuracy. This paper presents a method that quantifies necrosis in cell cultures by texture analysis of microscope images.

The image is divided into regions of equal size that are classified by means of a segmentation algorithm based on texture analysis into three categories: live cells, necrotic cells and background. The classification uses three discriminant functions, built from parameters derived from the histogram and the co-occurrence matrix and calculated by performing an initial stepwise discriminant analysis on 21 sample images from a training set.

The areas occupied by live and necrotic cells and number of live cells have been obtained for primary cellular cultures in intervals of 48 h during 2 weeks. The results have been compared with those obtained by an experienced observer, showing a very good correlation (Pearson's coefficient 0.95, kappa 0.87, $N = 1600$).

A method has been developed that provides an accuracy similar to that provided by an expert, while allowing a much higher number of fields to be counted.

Introduction

The rate of cell apoptosis is a significant parameter in many experiments involving cell cultures. Cell death kinetics can be measured by counting the number of cells and/or area occu-

Correspondence: M. Desco. Tel. + 34915866678; fax: + 34915868104; e-mail: desco@mce.hggm.es

pied on each culture dish, analysing images taken at different moments of their evolution. To obtain reliable statistics a large number of cells need to be counted, thus making the use of automatic procedures advisable.

Initially, the growing colonies yield high contrast images where the edges of the objects (individual cells) are rather conspicuous. As cell proliferation takes place, the size of the cells is reduced, noticeably increasing the density of cells as they begin to completely fill the plate. On the other hand, apoptosis leads to condensation and fragmentation of cell bodies, producing regions populated with unstructured smaller objects.

Several staining methods for measuring apoptosis are currently well established. DNA-binding dyes are frequently used, such as propidium iodide (PI) or Hoechst dye, terminal deoxynucleotidyl transferase (TdT)-mediated end-labelling of the DNA strand breaks (Gavrieli *et al.*, 1992), detection of phosphatidyl serine on apoptotic cell membranes with Annexin V (Vermes & Haanen, 1994), DNA fragmentation laddering on agarose gels, or direct visualization of apoptotic cells under the microscope. In addition, flow cytometry offers a variety of possibilities to measure apoptosis, either staining in the cell surface or intracellularly (Strebel *et al.*, 2001).

In theory, an appropriate segmentation algorithm (i.e. border detection, followed by cell classification) could accurately obtain the number of cells by identifying and classifying each cell type on phase-contrast microscope images. The main difficulty for individual cell segmentation arises from cell aggregation, which hinders the detection of the cell contours. This is a difficult task for most image-processing algorithms and the authors know of no successful attempt.

Some papers have been published on the quantification of the dynamics of cell colonies. In Proffitt *et al.* (1996), a system to measure relative cell numbers in culture plates was presented. Total fluorescence was used as a measure of the

number of cells per plate, after background fluorescence reduction. Boezeman *et al.* (1997) presented a method for automatic enumeration of proliferating bone marrow progenitors, by means of high pass filtering and morphological processing based on the circularity of cells. Some studies have also focused on the segmentation of clustered nuclei in fluorescent-stained samples (Garbay *et al.*, 1986; Ahrens *et al.*, 1990; Lockett & Herman, 1994; Malpica *et al.*, 1997). These methods are not expected to offer good results in the type of cultures studied in our work, as separation of individual cells is not straightforward when dead cells loose their shape and size properties.

In Kong & Ringer (1995) a system for apoptosis detection by image analysis was proposed, using a counterstain for nuclei detection and a stain to detect apoptotic nuclei. Matthews *et al.* (1998) developed a system to detect apoptosis using staining methods that detect apoptotic morphology.

Methods based on texture analysis are receiving increasing interest, and they have been used successfully to identify neoplastic nuclei by characterizing chromatin structure in breast tumours (Weyn *et al.*, 1998; Wouwer *et al.*, 2000) and in prostate cancer (Yogesan *et al.*, 1996), and to segment chromatin regions (Beil *et al.*, 1995).

This paper presents an automatic method developed for cell counting by characterizing the texture of regions in phase-contrast images without staining. The system allows the measure of confluence, or degree of coverage of the plate with cells. The use of phase contrast microscopy allows for *in vivo* studies, therefore not introducing experimental artefacts derived from staining or fixation.

Texture parameters have been extracted from a set of training samples, calculating the optimum set of discriminant functions by stepwise procedures. The procedure and a comparison with manual counting are presented.

Materials and methods

The automatic counting procedure comprises two steps. First, regions are classified as pertaining to any of the cell classes (dead or alive) or to the background. Then the total number of live cells is calculated using an estimation of the average cell size.

Segmentation of the image is performed by classifying each region into one of three a priori classes, on the basis of a vector of texture parameters computed for each region. These texture parameters were obtained from a training set of images by means of stepwise discriminant analysis that also provided the corresponding discriminant (Fisher) functions. Regions were assigned to a class, on the basis of texture parameters computed on wider window. Statistical analysis of textures is described below.

In order to calculate the number of live cells, their average size is introduced either directly or by using an interactive tool that estimates this average size by manually outlining several

cells. The area corresponding to live cells divided by average cell size provides an estimation of the number of cells.

Texture features

Texture parameters used in this application can be classified into first-order statistics, computed from the histogram, and second-order statistics, computed using the Gray Level Co-occurrence matrix (GLCM) (Haralick *et al.*, 1973). Mathematical expressions of the parameters and implementation details are provided in the Appendix.

The number of features extracted from the histogram (four features) and from the GLCM (11 features) at each of the four orientations and five distances used is too large. A reduction in the dimensionality of the features vector is required (Brady & Xie, 1996).

A subset including the most discriminant variables was selected by means of a stepwise discriminant analysis, using an input/output F-test to add and remove variables. The F-test is based on Wilk's lambda, which measures the ratio of the variance in each group and the total variance (Dillon & Goldstein, 1984). At each step, the variable that minimizes lambda, considered together with previously selected variables, is chosen. Independence among variables is assessed using tolerance. Tolerance of a variable X_j to variables $X_1, \ldots, X_{j-1}, \ldots X_p$ is defined as $Tol_j = 1 - R_j^2$ where R_j is the multiple correlation coefficient among X_j and variables $X_1, \ldots, X_{j-1}, \ldots X_p$ (Dillon & Goldstein, 1984). At each step, variables are added or eliminated depending on their partial F value. The procedure ends when no more variables can be entered or removed. The F to enter and F to remove values used were 3.84 and 2.71, respectively.

Classification by discriminant analysis

Once the most discriminant set of parameters is obtained, linear discriminant functions are calculated to automatically classify each sample into one of the three predefined groups.

In discriminant analysis (Keckla, 1988) a linear combination of the independent variables (textural features in our case) is formed, and this serves as the basis for classifying cases. We use linear discriminant or Fisher functions, of the following form:

$$D_s = B_{s1}X_1 + \ldots + B_{sp}X_p + B_{s0}$$

where $X_1, \ldots, X_p$ are the quantitative independent variables and $B_{s0}, B_{s1}, \ldots, B_{sp}$ are the weighting factors (Fisher coefficients) estimated from the data. These factors are chosen so that the ratio of the between-class sum of squares to the within-class sum of squares is as large as possible.

Training of the system was carried out only once and the resulting parameters were used throughout the rest of the experiments.
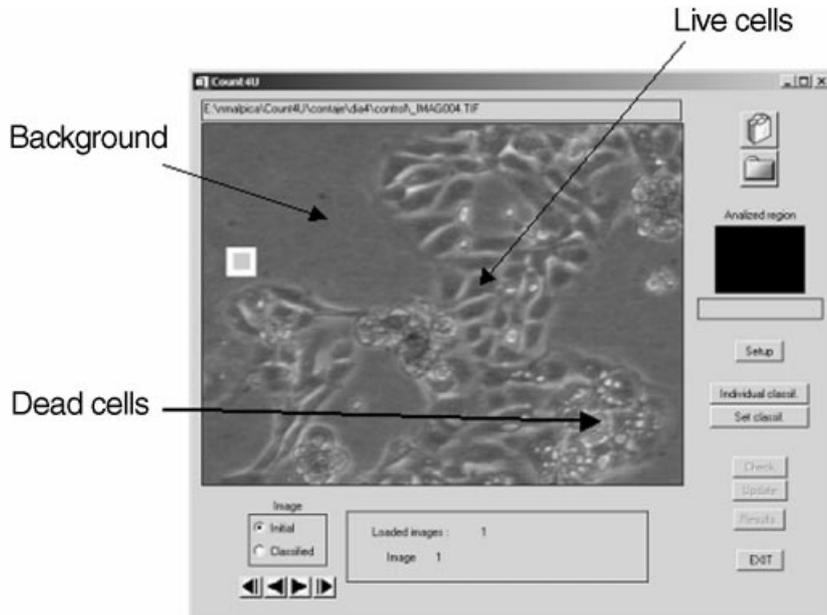
Fig. 1. User interface of the application. Regions of different classes are shown in the image, as well as the sizes of regions used for parameter calculation and classification, respectively.

Robustness assessment

The leave-one-out method was used to obtain an initial estimate of the correct classification rate. This method involves leaving out each case in turn, calculating the function based on the remaining cases, and then classifying the left-out case. The robustness of the discriminant functions was also assessed by jack-knifing: 10% of samples were taken out and the discriminant functions were estimated from the rest of the samples. All procedures for feature selection and discriminant function calculations were carried out using SPSS (SPSS Inc., Chicago, IL, USA).

Image analysis tool

The segmentation method was implemented in a complete end-user application, using IDL language (Research Systems Inc., Boulder, CO, USA). The user interface of the tool is shown in Fig. 1. It allows single images or a complete set of images to be loaded. After automatic classification, the user can interactively correct the assignment of any region if needed. Final results can be saved to an ASCII file for further analysis. Results showing the total surface for each class and the number of live cells are provided as output.

Experimental setting

The proposed method was tested in cell cultures using a previously established setting for the induction of cell death by means of two immunosuppressors with known cytotoxic activity, as previously reported (Hortelano *et al.*, 2000). The experiment consists of adding two immunosuppressors (CSA and Tacrolimus, FK506) to different primary cultures of renal cells, for measuring cell death kinetics. A third culture with no immunosuppressor is used as control. All experiments are performed on primary cell cultures from swine. Proximal tubule suspensions were obtained from collagenase digestion of the renal cortex and isopicnic centrifugation on 45% Percoll gradient (Tejedor *et al.*, 1988) and plated in plastic culture dishes (60 mm). Kinetics of culture with CSA were compared to cultures with no immunosupresor and to cultures with FK506, as a positive control. Cultures were incubated at 37 °C in a 95% air/5% CO_2 atmosphere. CSA was obtained from Sandimmun® (Novartis, Basel, Switzerland) and FK506 from Prograf® (Fujisawa, Tokyo, Japan). Cells were allowed to grow in the presence of CSA, FK506 or vehicle (control conditions) from zero time (eight dishes per treatment).

Phase contrast images were acquired with an Olympus IX70 microscope (Olympus Gmbh, Hamburg, Germany) with 40× magnification, and captured with a Sony DXC 151P colour CCD camera (Sony Ltd, Tokyo, Japan). Monochrome (8 bits pixel^{-1}) 736×560 pixel images were transferred to a Pentium III computer for analysis using a Matrox Meteor II frame grabber (Matrox Electronic Systems, Dorval, Canada).

Cultures were maintained for approximately 15 days; during this period images were obtained every 2 days, starting from day four. Three different dishes per treatment were chosen randomly. From each of them, seven images were obtained. Figure 2 shows images of the culture on the fourth and eleventh day of the study. The objective of the method is to segment the regions containing live cells, dead cells and the areas with no cells. Regions 32×32 pixels in size were assigned to a class, on the basis of texture parameters computed on a 60×60 window.

Two different sets of images were used, one for training and another for evaluation of the classification performance.
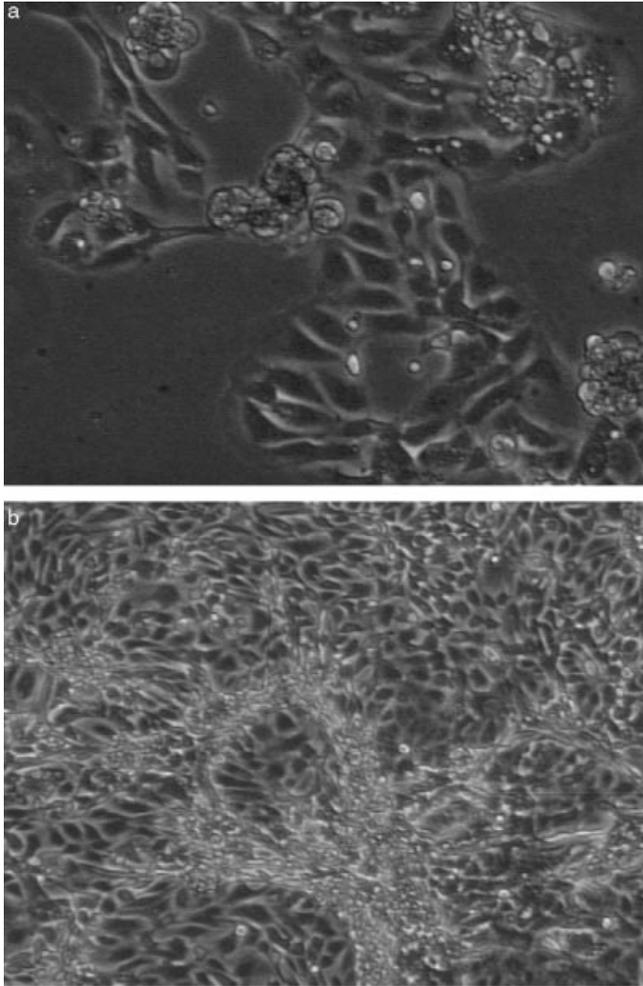
Fig. 2. Images of the cell culture on day 4 (a) and day 11 (b).

To select the most discriminant texture parameters and to establish the discriminant functions, a training set of 21 images (seven per type of culture) was obtained for each of the 5 days of study, as explained above. From them, 222 regions of interest were extracted. Each region was manually classified as formed by live cells, dead cells or background (dish). For each region, all the histogram and co-occurrence matrix parameters were computed. Co-occurrence matrices for $d = 1$, 2, 3, 4, 5 and $\theta = 0°, 45°, 90°, 135°$ were used (see Appendix). The classification rate obtained on the training set of regions was measured using a leave-one-out method. The robustness of the discriminant functions was assessed by jack-knifing, performing 10 different runs, randomly excluding 10% of the regions in each.

In order to assess the reliability of the results of the automatic method, segmentation (region classification) and cell counting were evaluated separately.

The agreement in region classification was assessed by considering the number of rectangular windows that were correctly classified in a set of four randomly chosen images corresponding to four different days. After the automatic classification, each image becomes divided into 400 regions (i.e. 1600 regions in total) and results are compared to the manual classification obtained by a experienced observer (Table 2), blind to the automatic result.

The rate of agreement is computed as:

$$p_o = \frac{Number\ of\ agreements}{Total\ number\ of\ regions}$$

This rate of agreement between different image classification methods can be considered as a reliability index in which a number of targets (image regions) are rated (classified) by different judges (methods). However, part of this agreement could be due to chance only. Even in the case when both ratings were independent of each other, a certain degree of random agreement would be present. For this reason, another measurement of reliability, known as the kappa coefficient (κ), has been used. Kappa is a chance-corrected measurement of agreement, defined by Bartko (1995):

$$kappa = \frac{p_o - p_e}{1 - p_e}$$

where p_o is the observed percentage of agreement between two methods and p_e is the agreement that would occur by chance. Random agreement can be measured by supposing that both measurements are independent. The number of regions classified into each class by each of the methods is plotted on Table 2.

The expected number of classifications into class i and j by each of the methods, respectively, assuming independence, is:

$$Expected\_cases:\ e_{ij} = \frac{(Row\ total)_i \times (Column\ total)_i}{Total\ number\ of\ cases}$$

Random coincidences are then $e_{11} + e_{12} + e_{13}$. Expected agreement can then be computed as: $p_e = (e_{11} + e_{22} + e_{33})/n$, where n is the total number of observations.

To evaluate the results of cell counting, 15 images were selected randomly, from which the area occupied by cells of each type and the number of live cells was computed both manually and automatically. Correlation is not always the best approach to compare two methods of measurement, as it does not measure the agreement between two variables, but the strength of a relation between them. If the results of both methods are plotted against each other, there will only be perfect agreement if the points lie along the line of equality; however, there will be perfect correlation when the points lie along any straight line. Altman (1991) proposed plotting the differences between both methods against their mean. The lack of agreement can then be assessed by the bias, estimated by the mean difference (d) and the standard deviation of the differences (s). In our case, we have used the results of the manual method instead of the average, as it represents the gold standard.

Results

Stepwise discriminant analysis resulted in the selection of 12 parameters. Parameter names and their weighting coefficients for the three linear discriminant functions are shown in Table 1. The leave-one-out method yielded a 100% classification success rate on the training set.

Region classification was evaluated by measuring the rate of agreement and the kappa index, as described in Materials and Methods. Table 2 shows the result of classification of the test regions. A rate of agreement of 0.94 was obtained, with a kappa of 0.87. Evaluation of the measured cell area and number of cells was performed as described above.

Taking the figures obtained manually as the standard, the relative difference (bias) is defined as:

$$Diff = \frac{(Automat.\ count - Manual\ count)}{Manual\ count}$$

From the experiments, the overall relative mean difference in live cells area was 0.2%, with a standard deviation of 6.8% (not significantly different from 0).

Table 1. Discriminant parameters and their weights in each discriminant function. Parameter names are explained in the Appendix. Numbers in parenthesis indicate neighbour distances in pixels along the *x* and *y* axes for co-occurrence matrix computation. See Appendix for the definition of texture parameters.

	Live cells	Dead cells	Dish
Percentile 99%	−0.964	−1.045	−0.691
InvDfMom(1,0)	30 551	30 603	31 107
Entropy(1,0)	19 650	19 784	19 777
AngScMom(1,-1)	−18 022	−17 895	−20 953
InvDfMom(1,-1)	1120	863	1301
AngScMom(2,0)	18 984	18 904	22 024
InvDfMom(2,0)	−1067	−940	−1737
InvDfMom(4,-4)	− 4059	−4382	−4492
SumEntrp(5,0)	−12 746	−12 708	−12 486
Contrast(5,5)	15	14	16
Entropy(5,5)	−2738	−2817	−3014
InvDfMom(5,-5)	5604	5993	6175
Constant	−15 811	−15 858	−16 042

Table 2. Comparison between manual and automatic classification of segmented regions. Each cell shows the number of regions in each class according to each method.

Manual classification	Automatic classification			
	Live cells	Dead cells	Background	Total
Live cells	1069	29	26	1124
Dead cells	33	269	5	307
Background	3	1	165	169
Total	1105	299	196	1600

Regarding cell counting, a relative mean difference of 18.06% and a standard deviation of 19.11% were obtained (not significantly different from 0).

Training was only carried out once, taking 3 h, and results were used for all experiments. The time needed to classify a single image was 29 s on a Pentium III 700 MHz PC. The average time taken by an experienced observer is 3 min.

Discussion

The method proposed provides quantitative figures (area of live and dead cells and number of live cells) similar to those obtained by an experienced observer. The results of region classification were better than those of cell counting. This may be due to the fact that the calculated number of cells requires an estimate of the average cell size. Cell sizes may differ significantly, especially in images taken after a few days of growth, as shown in Fig. 2. Although the interobserver variability is very small, the final result of cell counting strongly depends on the particular selection of cells performed by the user for average size calculation.

Focusing and image acquisition were performed manually in the present study. We have not studied the possible influence of defocusing on texture parameters. In any case, several precise methods for autofocusing are available (Santos *et al.*, 1997), which could easily be included as part of the procedure. In a completely automated setting, illumination should also be calibrated and controlled, even though most of the features used for classification are illumination invariant.

In the present study, the parameter estimation window was of a fixed size, which was determined empirically. The method uses only histogram and grey-level co-occurrence matrix parameters. Analysis windows must be large enough to have a sufficient number of values for parameter computing. The size of the classification window, those pixels that are assigned to a certain class, determines the resolution of the classification. Using a smaller window increases the resolution but also the computational cost. The system developed could be used to segment cultures of other different cell types, although the parameter selection and discriminant function calculation would have to be repeated for the new image types.

A reliable and easy to implement method has been developed, providing *in vivo* quantitative results on phase contrast microscopy images of cell cultures. The method has been evaluated using an independent data set. The system avoids any artefacts derived from staining and fixation, without even a requirement to open the dishes. Preliminary results show an accuracy similar to that provided by an expert, while allowing a much larger number of fields to be counted.

analysis software, in the framework of the EU COST B11 project. This work was partially funded by III PRICIT (Comunidad de Madrid).

References

Ahrens, P., Schleicher, A., Zilles, K. & Werner, L. (1990) Image analysis of Nissl-stained neuronal perikarya in the primary visual cortex of the rat: automatic detection and segmentation of neuronal profiles with nuclei and nucleoli. *J. Microsc.* **157**, 349–365.

Altman, D.G. (1991) Statistical analysis of comparison between laboratory methods. *J. Clin. Pathol.* **44**, 700–701.

Bartko, J.J. (1995) Measurement and reliability: Statistical thinking considerations. *Schizophrenia Bull.* **17**, 147–161.

Beil, M., Irinopoulou, T., Vassy, J. & Wolf, G. (1995) A dual approach to structural texture analysis in microscopic cell images. *Computer Meth. Programs Biomedicine*, **48**, 211–219.

Boezeman, J., Raymakers, R., Vierwinden, G. & Linssen, P. (1997) Automatic analysis of growth onset, growth rate and colony size of individual bone marrow progenitors. *Cytometry*, **28**, 305–1310.

Brady, M. & Xie, Z.-Y. (1996) Feature selection for texture segmentation. *Advances in Image Understanding* (ed. by K. Bowyer and N. Ahuja), pp. 29–44. Wiley, New York.

Dillon, W.R. & Goldstein, M. (1984) *Multivariate Analysis*. John Wiley & Sons, New York.

Garbay, C., Chassery, J.M. & Brugal, G. (1986) An interactive region growing process for cell image segmentation based on local color similarity and global shape criteria. *Anal. Quantit. Cytol. Histol.* **8**, 25–34.

Gavrieli, Y., Sherman, Y. & Ben-Sasson, S. (1992) Identification of programmed cell death *in situ* via specific labeling of nuclear DNA fragmentation. *J. Cell Biol.* **119**, 493–501.

Haralick, R., Shanmugam, K. & Dinstein, I. (1973) Textural features for image classification. *IEEE Trans. Systems, Man. Cybernetics*, **3**, 610–621.

Hortelano, S., Castilla, M., Torres, A.M., Tejedor, A. & Bosca, L. (2000) Potentiation by nitric oxide of cyclosporin A and FK506-induced apoptosis in renal proximal tubule cells. *J. Am. Soc. Nephrol.* **11**, 2315–2323.

Keckla, W.R. (1988) *Discriminant Analysis: Quantitative Applications in the Social Sciences*. Sage Publications, London.

Kong, J. & Ringer, D.P. (1995) Quantitative *in situ* image analysis of apoptosis in well and poorly differentiated tumors from rat liver. *Am. J. Pathol.* **147**, 1626–1632.

Lockett, S.J. & Herman, B. (1994) Automatic detection of clustered, fluorescent-stained nuclei by digital image-based cytometry. *Cytometry*, **17**, 1–12.

Malpica, N., Ortiz, C., Vaquero, J.J., Santos, A., Vallcorba, I., García-Sagredo, J.M., Pozo, F. & d. (1997) Applying watershed algorithms to the segmentation of clustered nuclei. *Cytometry*, **28**, 289–297.

Matthews, J.B., Harrison, A., Palcic, B. & Skov, K. (1998) Automated fluorescence microscopic measurement of apoptosis frequency following ionizing radiation exposure in cultured mammalian cells. *Int. J. Radiation Biol.* **73**, 629–639.

Proffitt, R.T., Tran, J.V. & Reynolds, C.P. (1996) A fluorescence digital image microscopy system for quantifying relative cell numbers in tissue culture plates. *Cytometry*, **24**, 204–213.

Santos, A., Ortiz, C., Vaquero, J.J., Peña, J.M., Malpica, N. & Pozo, F.d. (1997) Evaluation of autofocus functions in molecular cytogenetic analysis. *J. Microsc.* **188**, 264–272.

Strebel, A., Harr, T., Bachmann, F., Wernli, M. & Erb, P. (2001) Green fluorescent protein as a novel tool to measure apoptosis and necrosis. *Cytometry*, **43**, 126–133.

Tejedor, A., Noel, J., Vinay, P., Boulanger, Y. & Gougoux, A. (1988) Characterization and metabolism of canine proximal, thick ascending limbs and collecting duct tubules in suspension. *Can. J. Physiol. Pharmacol.* **66**, 997–1009.

Vermes, I. & Haanen, C. (1994) Apoptosis and programmed cell death in health and disease. *Adv. Clin. Chem.* **31**, 117–246.

Weyn, B., Wouwer, G.V.D., Van Daele, A.V., Scheunders, P., Van Dyck, D.V., Van Marck, E.V. & Jacob, W. (1998) Automated breast tumor diagnosis and grading based on wavelet chromatin texture description. *Cytometry*, **33**, 32–40.

Wouwer, G.V.D., Weyn, B., Scheunders, P., Jacob, W., Marck, E.V. & Dyck, D.V. (2000) Wavelets as chromatin texture descriptors for the automated identification of neoplastic nuclei. *J. Microsc.* **197**, 25–35.

Yogesan, K., Jorgensen, T., Albregtsen, F., Tveter, K.J. & Danielsen, H.E. (1996) Entropy-based texture analysis of chromatin structure in advanced prostate cancer. *Cytometry*, **24**, 268–276.

Appendix

Texture parameters

A first group of parameters is computed from the normalized grey-level histogram. The normalized histogram is the probability density function for the grey levels of a specific region. If we denote by $p(z_i)$ the probability of each grey value z_i, the following parameters can be defined:

$$\text{Mean: } \mu = \sum_{z_i=0}^{N-1} z_i p(z_i)$$

$$\text{Variance: } \sigma^2 = \sum_{z_i=0}^{N-1} (z_i - \mu)^2 p(z_i)$$

$$\text{Skewness: } \mu_3 = \sigma^{-3} \sum_{z_i=0}^{N-1} (z_i - \mu)^3 p(z_i)$$

$$\text{Kurtosis: } \mu_4 = \sigma^{-4} \sum_{z_i=0}^{N-1} (z_i - \mu)^4 p(z_i) - 3$$

The histogram considers the grey level of each pixel separately and no spatial information is conveyed in these parameters. To incorporate spatial distribution of the grey levels we make use of the grey-level co-occurrence matrix (GLCM). Any GLCM element $P_d(i,j)$ reflects the distribution of the probability of occurrence of a pair of grey levels (i,j) separated by a given distance d. The GLCM is computed by mapping the grey-level co-occurrence probabilities based on spatial relations of pixels in different angular directions θ.

As with the histogram, a normalized version of the co-occurrence matrix can be computed, dividing each element by the total number of neighbours for each d and θ. These values depend on the texture.

From the co-occurrence matrix, the following parameters were derived:

Second order angular moment: $AngScMom = \displaystyle\sum_{z_i=0}^{N-1} \sum_{z_i=0}^{N-1} [p(z_i,z_j)]^2$

Contrast: $Contrast = \displaystyle\sum_{z_i=0}^{N-1} \sum_{z_i=0}^{N-1} (z_i - z_j)^2 p(z_i,z_j)$

Correlation: $Correlat = \displaystyle\sum_{z_i=0}^{N-1} \sum_{z_j=0}^{N-1} \dfrac{z_i z_j p(z_i,z_j) - \mu_x \mu_y}{\sigma_x \sigma_y}$

Sum of squares: $SumOfSqs = \displaystyle\sum_{z_i=0}^{N-1} \sum_{z_i=0}^{N-1} (z_i - \mu_x)^2 p(z_i,z_j)$

Inverse Difference Moment: $InvDfMom = \displaystyle\sum_{z_i=0}^{N-1} \sum_{z_i=0}^{N-1} \dfrac{p(z_i,z_j)}{1+(z_i-z_j)^2}$

Entropy: $Entropy = -\displaystyle\sum_{z_i=0}^{N-1} \sum_{z_j=0}^{N-1} p(z_i,z_j) \log[p(z_i,z_j)]$

Sum Average: $SumAverg = \displaystyle\sum_{z_i=0}^{2(N-1)} z_i \, p_{x+y}(z_i)$

$p_{x+y}(k) = \displaystyle\sum_{z_i=0}^{N-1} \sum_{z_j=0}^{N-1} p(z_i,z_j)$ where $z_i + z_j = k = 0,1,2,\dots,2(N-1)$

Sum variance: $SumVariance = \displaystyle\sum_{z_i=0}^{2(N-1)} (z_i - SumAverg) p_{x+y}(z_i)$

Sum Entropy: $SumEntrp = -\displaystyle\sum_{z_i=0}^{2(N-1)} p_{x+y}(z_i) \log(p_{x+y}(z_i))$

Difference variance: $DifVarnc = \displaystyle\sum_{z_i=0}^{2(N-1)} (z_i - \mu_{x-y})^2 p_{x-y}(z_i)$

where

$p_{x-y}(k) = \displaystyle\sum_{z_i=0}^{N-1} \sum_{z_j=0}^{N-1} p(z_i,z_j) 1/2 z_i - 1/2 = k = 0,1,2,\dots,N-1$

Entropy of difference: $DifEntrp = -\displaystyle\sum_{z_i=0}^{2(N-1)} p_{x-y}(z_i) \log(p_{x-y}(z_i))$

In these expressions, N is the number of grey levels, z_i are the different grey levels, $p(z_i,z_j)$ is the value of the GLCM at point (i,j), μ_x is the mean value of GLCM values accumulated in the x direction and μ_{x-y} is the mean value of the distribution p_{x-y}.

To improve computation speed, advantage can be taken from the fact that the co-occurrence matrix is symmetric. On the other side, the size of the GLCM depends on the grey level resolution of the image. Texture parameters have shown to be reasonably invariant to grey-level quantization. In this work, images were quantized to 4 bits pixel^{-1} before the matrix was calculated, to increase computational speed, and GLCM was computed for $d = 1, 2, 3, 4, 5$ and $\theta = 0°, 45°, 90°, 135°$.